Phase Equilibrium Measurements of Hydrogen−Tetrahydrofuran and Hydrogen−Cyclopentane Binary Clathrate Hydrate Systems

Hiroyuki Komatsu,[†] Hiroki Yoshioka,[†] Masaki Ota,[‡] Yoshiyuki Sato,[‡] Masaru Watanabe,[‡] Richard L. Smith, Jr.,*[,†,‡] and Cor J. Peters[§,||]

Graduate School of Environmental Studies, Tohoku University, Aoba-6-6-11, Aramaki Aza, Aoba-ku, Sendai 980-8579 Japan, Research Center of Supercritical Fluid Technology, Tohoku University, Aoba-6-6-11, Aramaki Aza, Aoba-ku, Sendai 980-8579 Japan, Laboratory of Process Equipment, Department of Process and Energy, Faculty of Mechanical, Maritime and Materials Engineering, Delft University of Technology, Leeghwaterstraat 44, 2628 CA Delft, The Netherlands, and Chemical Engineering Program, Petroleum Institute, Bu Hasa Building, Room 2203, P.O. Box 2533, Abu Dhabi, United Arab Emirates

Phase equilibrium data for H_2 + tetrahydrofuran (THF) and H_2 + cyclopentane (CP) binary clathrate hydrate systems were determined from temperature and pressure measurements with a newly designed semimicro ($\approx$ 0.78 cm^3) cell. The range of conditions studied for the two systems was at pressures from (2 to 14) MPa and at temperatures from (278 to 285) K. Inclusion characteristics of the hydrogen molecules for both systems were similar according to their Raman spectra. The measured data for the H_2 + THF binary clathrate hydrate system were in agreement with some of the data in the literature. New phase equilibrium data and Raman spectroscopy analyses for the H_2 + CP binary clathrate hydrate system are reported. The dissociation enthalpies determined from data in the pressure range from (8 to 14) MPa were (212 and 220) $kJ \cdot mol^{-1}$ for the H_2 + THF and H_2 + CP binary clathrate hydrate systems, respectively.

Introduction

The stability and structure of clathrate hydrates depend on the guest molecules in the cavity of their cages that are composed of hydrogen-bonded water molecules. Pure hydrogen hydrate forms structure II at high pressures ($\approx$ 200 MPa)[1] because the molecular size of hydrogen is very small. To reduce the equilibrium pressure of H_2 clathrate hydrate for the purpose of storing hydrogen in technological applications, one method is to add a guest molecule that promotes the formation of stable structures that will allow hydrogen to be enclathrated at low pressures ($\approx$ 6 MPa).[2] Some proposed guest molecules for structure II clathrate hydrates are tetrahydrofuran (THF),[2,3] cyclopentane (CP),[4] tetrahydrothiophene,[5] and furan,[5] and those for structure H clathrate hydrates are 1,1-dimethylcyclohexane,[6] methyl *tert*-butyl ether,[6] and methylcyclohexane.[6] For the case of H_2 + THF binary clathrate hydrate, some reports have been made on the temperature and pressure conditions of its dissociation; however, there is much variation in the data.[2,7–10] Although phase equilibrium data are available for H_2 + THF binary clathrate hydrates at many conditions, data are scarce or unavailable for many H_2 + guest molecule binary clathrate hydrate systems.

CP is a nonpolar solvent and forms structure II clathrate hydrate spontaneously when mixed with water at the appropriate conditions.[11] The binary CP + H_2O system exhibits liquid−liquid equilibrium at ambient and subambient conditions.[12] Palmer reported that three-phase equilibrium exists for CP + H_2O in which there was a clathrate hydrate phase, a CP-rich liquid phase, and a water-rich phase at 280.9 K and at atmospheric pressure.[13] The data that have been reported on the H_2 + CP binary clathrate hydrate system are those presented as a conference work,[4] and those made by calorimetry measurements[14] that were published as this work were being prepared. In this work, we report data measured by following the phase boundaries according to their temperature−pressure behavior.

Hydrate formation is a crystallization process that occurs in quiescent systems, but can require strong agitation to promote initiation of the crystallization, especially for hydrophobic guest molecules such as CP. Strong agitation can promote and accelerate hydrogen clathration. In this work, we show the design of a cell that can be vigorously stirred relative to its contents which should help to promote H_2 contact with hydrate crystals. The apparatus was verified by measuring the phase equilibrium of the H_2 + THF binary clathrate hydrate system. New phase equilibrium data for the H_2 + CP binary clathrate hydrate system are reported. Inclusion characteristics of the both binary clathrate hydrate systems are analyzed with Raman spectroscopy.

Experimental Section

Materials. Hydrogen gas (99.99 %, Iwaki Suiso), THF without stabilizer (99.5 %, Wako Pure Chemical, Inc.), and CP (≥ 99 %, Aldrich) were used without further purification. Ultrapure water (5.5 $\mu S \cdot m^{-1}$) was made with a commercial apparatus for distilling water (RFD250NB, Advantec, Tokyo).

Apparatus. Figure 1 shows a schematic diagram of the experimental apparatus, and Figure 2 shows a cross-sectional view of the cell that is an original design of this work. The inner volume and maximum working pressure of the cell (Figure 2) were 0.78 cm^3 and 15 MPa, respectively. The cell (Figure 2) was fabricated out of 304 stainless steel and consisted of a seven-piece assembly that included a sapphire tube (14.0 mm o.d., 10.0 mm i.d., length 17.7 mm, Ogura Jewel Industry Co., Ltd.,

* Corresponding author: Tel.: +81-22-795-5863. Fax: +81-22-795-5864. E-mail: smith@scf.che.tohoku.ac.jp.
[†] Graduate School of Environmental Studies, Tohoku University.
[‡] Research Center of Supercritical Fluid Technology, Tohoku University.
[§] Delft University of Technology.
[||] Petroleum Institute.

10.1021/je900767h
Published on Web 01/07/2010

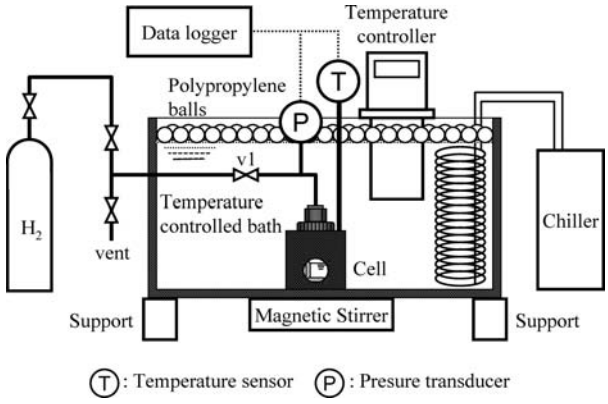

Figure 1. Schematic diagram of the experimental apparatus.

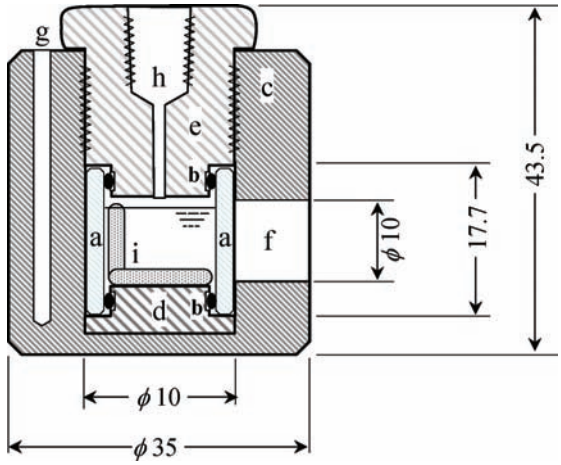

Figure 2. Cross-sectional view of the semimicro cell. Components: (a) sapphire tube, (b) o-ring, (c) outer housing, (d) lower support, (e) upper support gland nut, (f) view port, (g) thermowell, (h) hydrogen gas feed tube, (i) L-shape stirring bar. Cross-section is taken at 90° to allow view of the thermowell and one of the view ports. Dimensions are in millimeters.

Tokyo) which was held internally with two o-rings (NBR, JIS class 1B). The sapphire tube was maintained in a vertical position by a lower support and upper support gland nut that was held in an outer housing. The outer housing (Figure 2) had two diametrically opposed view ports (10 mm diameter) that allowed for visual observation of the cell contents. A stirrer was made by wrapping and pressing a 1.58 mm diameter stainless tube (1/16 in. 316 stainless steel) around a Teflon stirring bar (3 mm diameter × 8 mm long, rare-earth magnet, ≈ 0.4 kG) into a coiled L-shape (8.95 × 9.40 mm). The stirrer was interfaced to a magnetic stirrer (RP-1AR, Matsuura Seisakusyo, Ltd., Tokyo) that was outside of the temperature-controlled bath. The entire cell assembly was thermally insulated with Aeroflex sheet (Aeroflex, U.S.A.) and immersed in a temperature-controlled ethylene glycol + water (mole fraction ethylene glycol, 0.24) bath. The volume of gas space (Figure 1) between the cell and the valve (v1) along with volume of the pressure transducer was ≈ 2.05 cm^3 and was kept in the thermally controlled bath. The temperature of the bath was controlled with a refrigerated circulator controller (model MB, Julabo, Germany) and a chiller (CA-1112 type, Tokyo Rika Kikai Co., Ltd.). The bath was thermally insulated on the sides and bottom with Aeroflex sheet (Aeroflex, U.S.A.) and on the top with polypropylene balls (diameter, 10 mm, Matsuura Seisakusyo, Ltd., Tokyo) such that the temperature of the cell could be controlled to within ± 17 mK at 273.6 K. The system temperature was measured with a platinum resistance temperature sensor (Pt 100 Ω, 3.17 mm diameter (1/8 in.), NR-350, four-wire type, Netsushin) calibrated against a standard temperature probe (GE Kaye IRTD-400, stated uncertainty ± 25 mK) that had a stated uncertainty of 44 mK and was inserted into a hole in the cell assembly wall. The system pressure was measured by a sealed gauge pressure transducer (20 MPa F.S., PTX621-0, GE Sensing Japan) calibrated against a dead weight tester (Druck Pressurements M2200-5, stated uncertainty ± 0.015 %). The uncertainty in pressure measurement was 5.1 kPa.

Raman Spectroscopy Procedure. In a typical procedure, 0.0953 g of THF (2) and 0.4065 g of ultrapure water (1) were charged to the high-pressure cell that would give a THF mole fraction of $x_2 = 0.056$ and corresponded to a stoichiometric composition for structure II hydrate. The cell was purged with hydrogen gas five times at 8 MPa to reduce the air concentration to trace and was then pressurized to ≈ 13 MPa with hydrogen gas. Composition of the liquid was confirmed to undergo changes that reduced the organic mole fraction by 0.3 %. Final loaded mole fraction of the H_2O + THF system was $x_2 = 0.053$ THF with an estimated uncertainty of 0.1 %.

For CP (2) + H_2O (1), in a typical procedure, 0.0931 g of CP and 0.4069 g of ultrapure water were charged to the cell that gave a CP mole fraction of $x_2 = 0.056$ and is the stoichiometric composition for structure II hydrate. Through the purge procedure, the composition of the liquid was confirmed to undergo changes that reduced the organic compound mole fraction by 0.1 %. The final loaded mole fraction of the H_2O + CP system was $x_2 = 0.055$ CP with an estimated uncertainty of 0.1 %.

For either system, the temperature was maintained at 274 K, and binary clathrate hydrate was formed as the solution was stirred. The cell was moved into a freezer chest that was maintained at 253 K and was allowed to remain at this temperature for more than a day to ensure that the system had reached saturation occupancy with hydrogen. The H_2 + THF binary clathrate hydrate and H_2 + CP binary clathrate hydrates were analyzed by a laser Raman spectrophotometer with multichannel charge-coupled device (CCD) detector (NRS-2000c, JASCO, Tokyo). The argon ion laser used in the measurements had a wavelength of 514.5 nm and a radiant power of 100 mW. Spectral resolution was below 1 cm^{-1}. For the H_2 + THF binary clathrate hydrate, exposure times used to observe the C−C stretching vibrations and H−H stretching vibrations were (45 and 180) s, respectively. For the H_2 + CP binary clathrate hydrate, exposure times used to observe the C−C stretching vibrations and H−H stretching vibrations were (45 and 600) s, respectively. The longer time required for the H_2 + CP binary with respect to the H_2 + THF binary was needed to obtain a clear peak of the H−H stretching vibration.

Hydrate Phase Equilibrium Procedure. In measurements of either system, a sample was charged into the cell at the desired pressure using the experimental procedure described previously. The system temperature was maintained at 285 K (the H_2 + THF + water system) or 286 K (the H_2 + CP + water system) for 6 h as the solution was stirred. For either system, the temperature was lowered to about 274 K, and binary clathrate hydrate was formed. The system temperature was held constant until the system pressure stabilized.

In a typical set of measurements (Figure 3), the cell was step-heated by gradually increasing the temperature and allowing the pressure to stabilize. The system temperature and pressure stabilized rapidly and typically required 3 min. Much longer equilibration times were used as noted below. The step size of

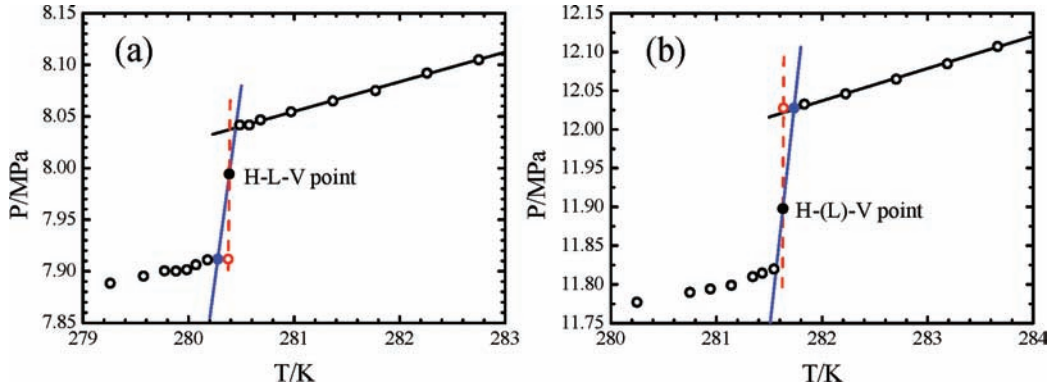

Figure 3. Typical pressure−temperature working plot for determining the hydrate dissociation pressure for the hydrogen + THF + water system. Symbols: black open circle (○), experimental data points; black solid circle (●) and blue solid circle, experimental data points used in the construction; red open circle, point used in construction for a hypothetical 0.1 K error in the step temperature giving a 0.07 K deviation in dissociation temperature and 0.004 MPa deviation in dissociation pressure. In (a), a clear three-phase, H−L−V point is observed. In (b), an incipient liquid phase, denoted as (L), is observed with the H−V phases.

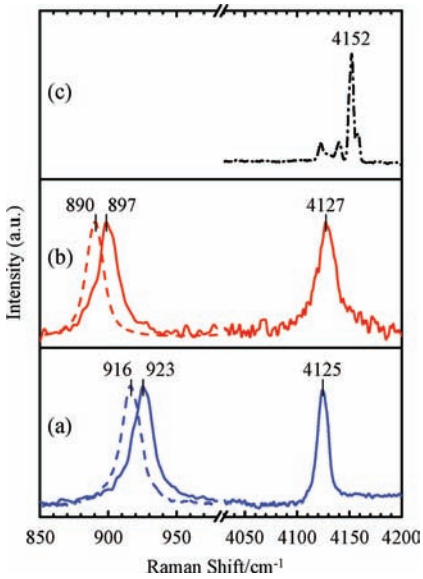

Figure 4. Raman spectra of (a) the hydrogen + THF system, (b) the hydrogen + CP system, and (c) hydrogen gas. Solid line, hydrate; dashed line, liquid; dash−dot−dashed line, gas.

the temperature increase was typically 0.1 K. After each temperature increase, pressure was allowed to equilibrate and to remain stable for at least 3 h, and in the vicinity of the hydrate dissociation temperature the equilibration time was typically 17 h. Points were noted on the hydrate−vapor (H−V), hydrate−liquid−vapor (H−L−V), and liquid−vapor (L−V) equilibrium curves as shown in Figure 3. The point of the hydrate dissociation was taken as the point at the intersection of the liquid−vapor (L−V) line and the hydrate−liquid−vapor (H−L−V) line as shown in Figure 3a. The temperature of hydrate dissociation was defined as the point of hydrate equilibria[15] and was determined from the intersection of the H−L−V equilibrium line with the L−V equilibrium curve (Figure 3a). In constructing the H−L−V line, a line was drawn between the H−L−V equilibrium point and the H−V equilibrium point adjacent to the H−L−V equilibrium point, because only one observed the H−L−V equilibrium point could generally be observed (Figure 3a). Working curves and constructions for each data point measured are given in the online material (Supporting Information). A hypothetical error of 0.1 K in the construction leads to an error in the dissociation pressure of 0.004 MPa (Figure 3b). Replicate experimental runs that allow for errors in loading procedure, composition, temperature, construction, and observed phenomena had a deviation in dissociation pressure of 0.018 MPa maximum (Supporting Information). Visual observations from the cell window were used to confirm the phase equilibria.

Table 1. Phase Equilibrium Data for the Hydrogen (1) + THF (2) + H_2O (3) Clathrate Hydrate System[a]

T/K	*P*/MPa
278.27	2.093
279.09	4.122
279.75	5.969
280.45	8.039
281.04	9.877
281.73	12.026
282.03	12.964

[a] The composition, $x_2 = 0.053$, refers to the 2 mole fraction of THF in the THF + H_2O mixture.

Table 2. Phase Equilibrium Data for Hydrogen (1) + CP (2) + H_2O (3) Clathrate Hydrate System[a]

T/K	*P*/MPa
280.70	2.463
281.35	4.344
281.63	5.125
282.34	7.254
282.87	9.050
283.24	10.194
283.46	11.132
284.02	13.116
284.31	14.005

[a] The composition, $x_2 = 0.055$, refers to mole fraction in the CP + H_2O mixture.

Results and Discussion

Raman Spectroscopy Analysis. The Raman spectra for the liquid and hydrate phases are shown for the H_2−THF−H_2O system (Figure 4a) and the H_2−CP−H_2O system (Figure 4b). Raman spectra for gaseous H_2 is shown in Figure 4c, where H−H stretching at 4152 cm^{-1} can be seen that is in accord with the literature.[2] The most prominent peaks in the H_2−THF−H_2O system (Figure 4a) were C−C stretching vibrations for THF liquid (916 cm^{-1}), C−C stretching vibrations for THF clathrate hydrate (923 cm^{-1}), and H−H stretching for H_2 in the clathrate hydrate (4125 cm^{-1}). The most prominent peaks in the H_2−CP−H_2O system (Figure 4b) were CP liquid (890 cm^{-1}), C−C stretching vibrations for CP clathrate hydrate (897 cm^{-1}), and H−H stretching for H_2 in the clathrate hydrate

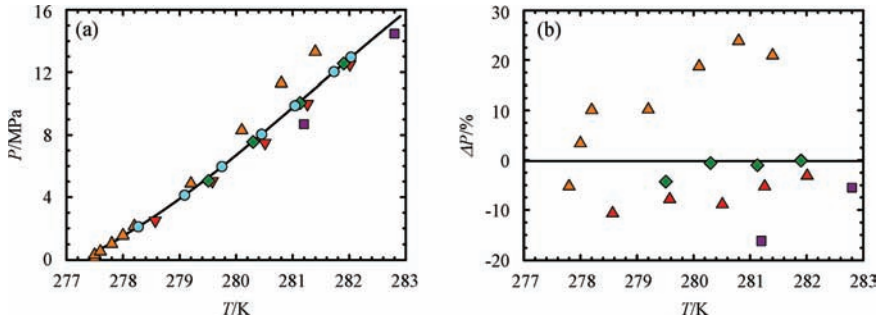

Figure 5. H_2 (1) + THF (2) + H_2O (3) clathrate hydrate system: (a) pressure−temperature diagram and (b) deviation plot from a polynomial equation in T/K fit to data in this work, $P = 644\,300 - 6875T + 24.440T^2 - 0.02895T^3$. THF composition is close to stoichiometric ($x_2 = 0.056$) for all data. Symbols: blue ●, $x_2 = 0.053$, this work; purple ■, $x_2 = 0.0556$, Anderson et al. (2007); orange ▲, $x_2 = 0.056$, Hashimoto et al. (2006); red ▼, $x_2 = 0.0579$, Peters et al. (2005); green ◆, $x_2 = 0.05$, Florusse et al. (2004).

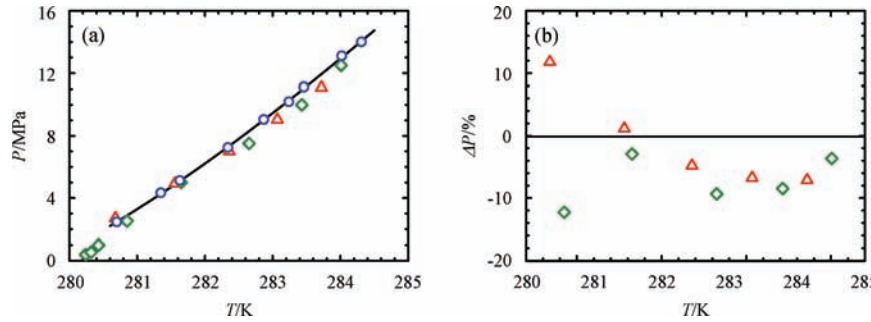

Figure 6. H_2 (1) + CP (2) + H_2O (3) clathrate hydrate system for various CP compositions, x_2: (a) pressure−temperature diagram and (b) deviation plot from a polynomial equation in T/K fit to data in this work, $P = 256400 - 2691T + 9.401T^2 - 0.01093T^3$. Symbols: blue ○, $x_2 = 0.055$, this work; red △, $x_2 = 0.223$, Zhang and Lee (2009); green ◇, $x_2 = 0.056$, Cruz Duarte et al. (2008).

(4127 cm^{-1}). These values were almost coincident with literature values[16,17] for the C−C stretching vibrations and were coincident with literature values[2] for the H−H stretching vibrations for the H_2−THF−H_2O system. Because Raman spectra for H_2 + CP binary clathrate hydrate have not been reported in the literature, values reported in this work cannot be compared with literature values. However, the tendencies of the Raman spectral shifts (Figure 4) for the enclathrated hydrogen in the H_2 + CP binary clathrate hydrate system were similar to those for the H_2 + THF binary clathrate hydrate system, which means that the inclusion characteristics of the enclathrated hydrogen molecules were similar for both systems.

Hydrate Phase Equilibrium Measurements. Phase equilibrium measurements made of the H_2 (1) + THF (2) + H_2O (3) clathrate hydrate system at $x_2 = 5.3$ % THF are given in Table 1 and are plotted with literature data in Figure 5. Among the results reported for the H_2 + THF binary clathrate hydrate system,[2,7,9,10] values reported in this work and those of Florusse et al.[2] and Peters et al.[10] were found to agree within 1 % and 9 %, respectively, in the pressure region above 6 MPa. In the pressure region above 6 MPa, the results in this work differed considerably from those of Hashimoto et al.[7] and Anderson et al.[9] as shown in Figure 5b. On the other hand, the results of Hashimoto et al.[7] and Anderson et al.[9] differ from each other by at least 30 %. It should be noted that these researchers used much larger equilibrium cells than in this work. The formation of stoichiometric THF clathrate hydrate is weakly dependent on the composition of THF subject to sufficient THF availability near the stoichiometric composition of THF,[18,19] which means that the variation in the results cannot be explained by the small differences in THF concentrations. Since our data were reproducible and showed deviations of 4 % maximum with result data measured by a different method, we judged our apparatus and procedure to be sufficient for obtaining reliable data.

Phase equilibrium data for the H_2 (1) + CP (2) + H_2O (3) binary clathrate hydrate system at $x_2 = 0.055$ are summarized in Table 2. Figure 6 shows the data measured in this work for the H_2 + CP binary clathrate hydrate system plotted together with literature values.[4,20] The data in this work deviated at the lower pressures (from 2 to 6 MPa) with literature values by a maximum of 12 % and less than 8 % at higher pressures (Figure 6b). The data of Zhang and Lee[14] were measured at high CP mole fractions, which could influence their analyses, since they used a calorimetric method. The data in this work agreed with the results of the literature to within (3 to 9) % above about 5 MPa (Figure 6b). At higher pressures, the data of Cruz Duarte et al.[4] show a distinct shift in the $p-T$ slope compared with those authors' low pressure data that should not be present without a phase change. The slope of the curve in this work was steeper than the slope of the p, T curve of Zhang and Lee.[14]

The dissociation temperatures and enthalpies of the two clathrate systems are discussed next. Comparing Figures 5 and 6, the region of stability for the H_2 + CP hydrate system is larger than that of the H_2 + THF hydrate system since its p, T curve occurs at higher temperatures. The dp/dT slopes (Figures 5 and 6) can be analyzed with a modified form of the Clausius−Clapeyron equation:[20]

$$\frac{\mathrm{d}\ln p}{\mathrm{d}(1/T)} = -\frac{\Delta_{\mathrm{dis}}H}{zR} \qquad (1)$$

where $\Delta_{\mathrm{dis}}H$ is the enthalpy of dissociation, R is the gas constant, and z is the compressibility factor that accounts for the nonideality of vapor phase. Figure 7 shows the dissociation data plotted as the logarithm of the pressure versus the inverse absolute temperature for the systems at pressures above 8 MPa. Average values of z for pure hydrogen were obtained from the National Institute of Standards and Technology (NIST) web-

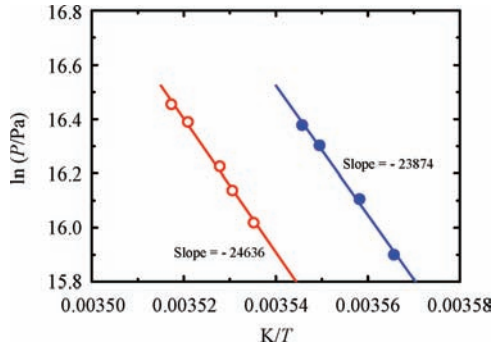

Figure 7. Hydrate dissociation line for H_2 (1) + THF (2) + H_2O clathrate hydrate system and the H_2 (1) + CP (2) + H_2O (3) clathrate hydrate system. Symbols: blue ●, the H_2 + THF ($x_2 = 0.053$) + H_2O system; red ○, the H_2 + CP ($x_2 = 0.055$) + H_2O system.

book[21] and were used in the data reduction over the pressure range of (8 to 14) MPa. The value of z used for the H_2 + THF clathrate hydrate system was 1.0673 (min 1.05, max 1.08), and that used for the H_2 + CP binary clathrate hydrate system was 1.0719 (min 1.06, max 1.09). The enthalpies of dissociation were determined to be (212 and 220) kJ·mol^{-1} for the H_2 + THF and H_2 + CP binary clathrate hydrate systems, respectively.

Conclusions

Phase equilibria for the H_2 + THF and the H_2 + CP binary clathrate hydrate systems were measured with a newly designed apparatus. The apparatus was confirmed with literature data of the H_2 + THF binary clathrate hydrate system. From the Raman spectroscopy, inclusion characteristics of the hydrogen molecules in the H_2 + CP binary clathrate hydrate were similar to those of the H_2 + THF binary clathrate hydrate. The dissociation enthalpies are similar for the H_2 + THF + guest and H_2 + CP + guest binary clathrate hydrate systems.

Supporting Information Available:

Figures S1 to S5. This material is available free of charge via the Internet at http://pubs.acs.org.

Literature Cited

(1) Mao, W. L.; Mao, H. K.; Goncharov, A. F.; Struzhkin, V. V.; Guo, Q. Z.; Hu, J. Z.; Shu, J. F.; Hemley, R. J.; Somayazulu, M.; Zhao, Y. S. Hydrogen clusters in clathrate hydrate. *Science* **2002**, *297*, 2247–2249.

(2) Florusse, L. J.; Peters, C. J.; Schoonman, J.; Hester, K. C.; Koh, C. A.; Dec, S. F.; Marsh, K. N.; Sloan, E. D. Stable low-pressure hydrogen clusters stored in a binary clathrate hydrate. *Science* **2004**, *306*, 469–471.

(3) Cruz Duarte, A. R.; Peters, C. J.; Zevenbergen, J. F. In *Kinetics of formation and dissociation of sII hydrogen clathrate hydrates*, The 6th International Conference on Gas Hydrates, Vancouver, British Columbia, Canada, July 6−10, 2008.

(4) Cruz Duarte, A. R.; Shariati, A.; Zevenbergen, J. F.; Florusse, L. J.; Peters, C. J. In *Hydrogen Storage in Clathrate Hydrates: Phase Equilibria, Thermodynamics and Kinetics*, 17th World Hydrogen Energy Conference (WHEC2008), Queensland, Australia, June 15−19, 2008.

(5) Tsuda, T.; Ogata, K.; Hashimoto, S.; Sugahara, T.; M., M.; Ohgaki, K. Storage capacity of hydrogen in tetrahydrothiophene and furan clathrate hydrates. *Chem. Eng. Sci.* **2009**, *64*, 4150–4154.

(6) Duarte, A. R. C.; Shariati, A.; Peters, C. J. Phase Equilibrium Measurements of Structure sH Hydrogen Clathrate Hydrates with Various Promoters. *J. Chem. Eng. Data* **2009**, *54*, 1628–1632.

(7) Hashimoto, S.; Murayama, S.; Sugahara, T.; Sato, H.; Ohgaki, K. Thermodynamic and Raman spectroscopic studies on H_2 + tetrahydrofuran plus water and H_2 + tetra-n-butyl ammonium bromide plus water mixtures containing gas hydrates. *Chem. Eng. Sci.* **2006**, *61*, 7884–7888.

(8) Hashimoto, S.; Sugahara, T.; Sato, H.; Ohgaki, K. Thermodynamic stability of H_2 + tetrahydrofuran mixed gas hydrate in nonstoichiometric aqueous solutions. *J. Chem. Eng. Data* **2007**, *52*, 517–520.

(9) Anderson, R.; Chapoy, A.; Tohidi, B. Phase relations and binary clathrate hydrate formation in the system H_2-THF-H_2O. *Langmuir* **2007**, *23*, 3440–3444.

(10) Peters, C. J.; Rovetto, L. J.; Schoonman, J. In *Phase behavior of low-pressure hydrogen clathrate hydrate*, 5th International Conference on Gas Hydrates, Trondheim, Norway, 2005; pp 1644−1650.

(11) Tohidi, B.; Danesh, A.; Todd, A. C.; Burgass, R. W.; Ostergaard, K. K. Equilibrium data and thermodynamic modelling of cyclopentane and neopentane hydrates. *Fluid Phase Equilib.* **1997**, *138*, 241–250.

(12) Maczynski, A.; Shaw, D. G.; Goral, M.; Wisniewska-Goclowska, B.; Skrzecz, A.; Maczynska, Z.; Owczarek, I.; Blazej, K.; Haulait-Pirson, M. C.; Kapuku, F.; Hefter, G. T.; Szafranski, A. IUPAC-NIST solubility data series. 81. Hydrocarbons with water and seawater - Revised and updated part 1. C-5 hydrocarbons with water. *J. Phys. Chem. Ref. Data* **2005**, *34*, 441–476.

(13) Palmer, H. A. *Characterization of hydrogen-type hydrates*. Ph.D. Thesis, University of Oklahoma, Norman, OK, 1950.

(14) Zhang, J. S.; Lee, J. W. Equilibrium of Hydrogen plus Cyclopentane and Carbon Dioxide plus Cyclopentane Binary Hydrates. *J. Chem. Eng. Data* **2009**, *54*, 659–661.

(15) Mooijer-van den Heuvel, M. M.; Peters, C. J.; Arons, J. D. Influence of water-insoluble organic components on the gas hydrate equilibrium conditions of methane. *Fluid Phase Equilib.* **2000**, *172*, 73–91.

(16) Prasad, P. S. R.; Prasad, K. S.; Thakur, N. K. Laser Raman spectroscopy of THF clathrate hydrate in the temperature range 90−300 K. *Spectrochim. Acta, Part A* **2007**, *68*, 1096–1100.

(17) Tkachev, S. N.; Pravica, M.; Kim, E.; Weck, P. F. Raman spectroscopic study of cyclopentane at high pressure. *J. Chem. Phys.* **2009**, *130*, 204505-1–204505-6.

(18) Otake, K.; Tsuji, T.; Sato, I.; Akiya, T.; Sako, T.; Hongo, M. A proposal of a new technique for the density measurement of solids. *Fluid Phase Equilib.* **2000**, *171*, 175–179.

(19) Delahaye, A.; Fournaison, L.; Marinhas, S.; Chatti, I.; Petitet, J. P.; Dalmazzone, D.; Furst, W. Effect of THF on equilibrium pressure and dissociation enthalpy of CO_2 hydrates applied to secondary refrigeration. *Ind. Eng. Chem. Res.* **2006**, *45*, 391–397.

(20) Sloan, E. D.; Koh, C. A. *Clathrate Hydrates of Natural Gases*, 3rd ed.; Marcel Dekker, Inc.: New York, 2008.

(21) Lemmon, E. W.; McLinden, M. O.; Friend, D. G. Thermophysical Properties of Fluid Systems In *NIST Chemistry WebBook, NIST Standard Reference Database Number 69*; Mallard, P. J. L. a. W. G., Ed.; National Institute of Standards and Technology: Gaithersburg, MD, 2009. http://webbook.nist.gov (accessed September 18, 2009).

Received for review September 22, 2009. Accepted December 7, 2009.

JE900767H